A meshless method for the two-dimensional extended Boussinesq equations

Wan-Rong Chou[#1], Chia-Cheng Tsai[*2], Tai-Wen Hsu[**3], Shih-Chun Hsiao[#4]

[#] *Department of Hydraulic and Ocean Engineering, National Cheng Kung University, Tainan, Taiwan*
1 University Road, Tainan 701, Taiwan.

[1]chouwanrong@gmail.com [4]schsiao@mail.ncku.edu.tw

[*] *National Kaohsiung University of Science and Technology*
142 Haijhuan Rd., Nanzih District, Kaohsiung 811, Taiwan.

[2] tsaichiacheng@mail.nkmu.edu.tw

[**] *Center of Excellence for Ocean Engineering (CEOE), National Taiwan Ocean University 2 Pei-Ning Road, Keelung 202, Taiwan.*

[3] twhsu@mail.ntou.edu.tw

***Abstract*— Coastal and offshore area are extremely dynamic regions. Near-shore wave current field affects the layout and design of hydraulic constructions. This paper focuses on establishing a new two dimensional (2D) Boussinesq model with a meshless method, using the local radial basis function collocation method (LRBFCM). The main concept of the LRBFCM is the interpolation function values which is only associated with the neighbouring nodes in the entire domain. The theoretical formulation has been conducted. In contrast to the fully dense matrices with the global methods, the localized approach results in sparse matrices, which could promote the computation efficiency. In the theory of Boussinesq equations (BEs), different types of BEs are relevant to different horizontal velocities and higher-order terms. The model would be implemented to solve ocean engineering, coastal engineering and harbor engineering related wave motion problems.**

***Keywords*—Boussinesq equations; LRBFCM; Predictor-corrector method; Wave simulation; Boundary condition**

I. INTRODUCTION

Waves in the transformation process encountered the wave deformation caused by structure and the coastal morphology and bottom topography. They present stronger nonlinear behaviour and very complicated motions. Boussinesq equations (BEs) are capable of providing the nonlinear wave propagation in the shallow water regions. The idea originated with Boussinesq (1872), who consider the weakly dispersive and nonlinear effects. Peregrine (1967) set equations for variable depth, and combine computers calculations with theory, firstly. Previous studies applied three numerical methods such as FDM (finite difference method), FEM (finite element method) and FVM (finite volume method). FDM is an approximate numerical method that converts a differential problem into an algebraic problem. Abbott et al. (1978) are first applied FDM to BEs. Afterwards, numerous authors used it (Madsen and Sørensen, 1992; Nwogu, 1993; Wei et al., 1995). The advantage of the FEM is that it is suitable to deal with complex boundaries; therefore, there are many related applications in BEs (Katopodes and Wu, 1987; Zelt and Raichlen, 1990; Li et al., 1999). Recently, an amount of analysis has been dedicated to the description of the use of FVM in BEs (Erduran et al., 2005; Cienfuegos et al., 2006; Tonelli and Petti, 2009) because FVM discretisation technique applicable to arbitrarily unstructured meshes. However, these methods are difficult to implement the problem and extremely time-consuming to generate the grid and compute. In order to overcome the problem of traditional numerical methods, the meshless method has been proposed.

Lately, a new class of numerical method, which does not need meshes but uses only a set of nodes to approximate the solution has been developed. Radial basis functions (RBFs) are usually used as the basis functions in these meshless methods. Kansa (1990a) first intensively studied these functions in multivariate data interpolation. The method was then extended to the solution of partial differential equations by Kansa (1990b). However, the global RBF collocation method (GRBFCM) usually results in ill-conditioned system matrix when higher resolutions are required, such as wave problems.

Therefore, a localization procedure has been proposed to transform the prescribed dense system matrices into sparse ones. Lee et al. (2003) first proposed the local RBF collocation method (LRBFCM) based on the multiquadric RBF (Hardy, 1971). The LRBFCM has been utilized to interdisciplinary fields, such as the solution of diffusion problems (Šarler and Vertnik, 2006), Darcy flow in porous media (Kosec and Sarler, 2008), macrosegregation phenomena (Kosec et al., 2011) and others. Tsai et al. (2015) using LRBFCM to approximate radiation boundary conditions. The main concept of LRBFCM is the interpolation function values only associated with the neighboring nodes in the entire domain. In contrast to the fully dense matrices with the global methods, the localized approach leads to sparse matrices, which could increase the computation efficiency.

In our study, we developed a messless numerical model based on extended Boussinesq equations (Nwogu, 1993). We use a fourth order predictor-correct scheme for time step and second order for spatial discretization.

II. GOVERNING EQUATION

The extended Boussinesq equations by Nwogu (1993) are given by

$$\frac{\partial \eta}{\partial t}+\nabla\cdot\left[(h+\eta)\mathbf{u}\right] + \nabla\cdot\left\{\left(\frac{z_\alpha^2}{2}-\frac{h^2}{6}\right)h\nabla(\nabla\cdot\mathbf{u})+\left(z_\alpha+\frac{h}{2}\right)h\nabla\left[\nabla\cdot(h\mathbf{u})\right]\right\}=0, \tag{1}$$

and

$$\mathbf{u}_t+g\nabla\eta+(\mathbf{u}\cdot\nabla)\mathbf{u} + \cdot z_\alpha\left\{\frac{z_\alpha}{2}\nabla(\nabla\cdot\mathbf{u}_t)+\nabla\left[\nabla\cdot(h\mathbf{u}_t)\right]\right\}=0, \tag{2}$$

where h is the water depth, g is gravitation acceleration, η is the surface elevation, $\mathbf{u}=(u_1,u_2)$ the horizontal velocity at an arbitrary depth z_α, $\nabla\equiv(\partial/\partial x,\partial/\partial y)$ is the horizontal gradient operator, t is the time.

Equations (1) and (2) can be alternatively written as

$$\eta_t=E(\eta,\mathbf{u}), \tag{3}$$

$$\mathbf{u}_t=\mathbf{F}(\eta,\mathbf{u})+\left[\mathbf{F}_1(\eta,\mathbf{u})\right]_t, \tag{4}$$

in which

$$E(\eta,\mathbf{u})=-\nabla\cdot\left\{(h+\eta)\mathbf{u}+a_1h^3\nabla(\nabla\cdot\mathbf{u})+a_2h^2\nabla\left[\nabla\cdot(h\mathbf{u})\right]\right\}, \tag{5}$$

$$\mathbf{F}(\eta,\mathbf{u})=-\mathrm{g}\nabla\eta-(\mathbf{u}\cdot\nabla)\mathbf{u}, \tag{6}$$

$$\mathbf{F}_1(\eta,\mathbf{u})=h\left[b_1h\nabla(\nabla\cdot\mathbf{u})+b_2\nabla\left[\nabla\cdot(h\mathbf{u})\right]\right], \tag{7}$$

where the constants a_1,a_2,b_1,b_2 are given by

$$a_1=\frac{z_\alpha^2}{2h^2}-\frac{1}{6};\ a_2=\left(\frac{z_\alpha}{h}+\frac{1}{2}\right);\ b_1=\frac{z_\alpha^2}{2h^2};\ b_2=\frac{z_\alpha}{h}. \tag{8}$$

III. NUMERICAL SCHEME

The local RBF collocation method (LRBFCM) is used to perform the spatial discretization. Here, the LRBFCM is a meshless numerical method. First, the considered geometry is discretized into N nodes of $\mathbf{y}_1$'s for solving the corresponding unknowns of η, u_1, and u_2 on those points. Note that the nodes should be located both in the computational domain and on its boundary as shown in Fig. 1.

Therefore, it is desirable to discretize the operators in (1) and (2) as

$$\mathcal{L}\begin{pmatrix}\eta(\mathbf{x})\\u_1(\mathbf{x})\\u_2(\mathbf{x})\end{pmatrix}\Bigg|_{\mathbf{x}=\mathbf{y}_1} =\left\{\mathcal{L}^\eta\eta(\mathbf{x})+\mathcal{L}^{u_1}u_1(\mathbf{x})+\mathcal{L}^{u_2}u_2(\mathbf{x})\right\}\Big|_{\mathbf{x}=\mathbf{y}_1} \approx\left[\mathcal{L}^\eta\right]_{1\times N}[\eta]_{N\times1}+\left[\mathcal{L}^{u_1}\right]_{1\times N}[u_1]_{N\times1}+\left[\mathcal{L}^{u_2}\right]_{1\times N}[u_2]_{N\times1}, \tag{9}$$

where

$$[\eta]_{N\times1}=\begin{bmatrix}\eta(\mathbf{y}_1)\\\eta(\mathbf{y}_2)\\\vdots\\\eta(\mathbf{y}_N)\end{bmatrix}, \tag{10}$$

$$[u_1]_{N\times1}=\begin{bmatrix}u_1(\mathbf{y}_1)\\u_1(\mathbf{y}_2)\\\vdots\\u_1(\mathbf{y}_N)\end{bmatrix}, \tag{11}$$

and

$$[u_2]_{N\times1}=\begin{bmatrix}u_2(\mathbf{y}_1)\\u_2(\mathbf{y}_2)\\\vdots\\u_2(\mathbf{y}_N)\end{bmatrix}, \tag{12}$$

are the approximated data and $\mathcal{L}$ is a linear differential operator of either the governing equations or the boundary condition depending on the location of $\mathbf{y}_i$.

Observing the governing equations of (3) and (4), four operators $\nabla\cdot\mathbf{u}$, $\nabla(\nabla\cdot\mathbf{u})$, $\nabla\eta$, and $\mathbf{u}\cdot\nabla\mathbf{u}$ should be considered for $\mathcal{L}$. For example, $\nabla\cdot\mathbf{u}$ can be presented as,

$$\nabla\cdot\mathbf{u}=\mathcal{L}^\eta\eta+\mathcal{L}^{u_1}u_1+\mathcal{L}^{u_2}u_2=\begin{pmatrix}0\\0\end{pmatrix}\eta+\begin{pmatrix}\frac{\partial}{\partial x_m}\end{pmatrix}u_1+\begin{pmatrix}\frac{\partial}{\partial x_n}\end{pmatrix}u_2, \tag{13}$$

where $m=1$ and $n=2$.

The second operator $\nabla(\nabla\cdot\mathbf{u})$ can be expressed as

$$\nabla(\nabla\cdot\mathbf{u})=\mathcal{L}^\eta\eta+\mathcal{L}^{u_1}u_1+\mathcal{L}^{u_2}u_2 =\begin{pmatrix}0\\0\end{pmatrix}\eta+\begin{pmatrix}\frac{\partial^2}{\partial x_m^{\,2}}\\\frac{\partial^2}{\partial x_m\partial x_n}\end{pmatrix}u_1+\begin{pmatrix}\frac{\partial^2}{\partial x_n^{\,2}}\\\frac{\partial^2}{\partial x_m\partial x_n}\end{pmatrix}u_2. \tag{14}$$

The third operator $\nabla\eta$ can be written as

$$\nabla\eta=\mathcal{L}^\eta\eta+\mathcal{L}^{u_1}u_1+\mathcal{L}^{u_2}u_2=\begin{pmatrix}\frac{\partial}{\partial x_m}\\\frac{\partial}{\partial x_n}\end{pmatrix}\eta+0u_1+0u_2. \tag{15}$$

The last operator $\mathbf{u}\cdot\nabla\mathbf{u}$ as

$$\mathbf{u}\cdot\nabla\mathbf{u}=\mathcal{L}^\eta\eta+\mathcal{L}^{u_1}u_1+\mathcal{L}^{u_2}u_2 =0\eta+\left(u_1\frac{\partial}{\partial x_m}+u_2\frac{\partial}{\partial x_n}\right)u_1+\left(u_1\frac{\partial}{\partial x_m}+u_2\frac{\partial}{\partial x_n}\right)u_2. \tag{16}$$

Once an operator $\mathcal{L}^{\phi}$ is given, it is required to have a local RBF approximation as

$$\mathcal{L}^{\phi}\phi \approx \left[\mathcal{L}^{\phi}\right]_{1\times K}\left[\phi\right]_{K\times 1}, \tag{17}$$

where

$$\left[\phi\right]_{K\times 1} = \begin{bmatrix} \phi(\mathbf{y}_1) \\ \phi(\mathbf{y}_2) \\ \vdots \\ \phi(\mathbf{y}_K) \end{bmatrix}, \tag{18}$$

is the approximated data with ϕ being one of the dependent variable η, u_1, and u_2. In addition, $\left[\mathcal{L}^{\phi}\right]_{1\times K}$ are the coefficients to be introduced in the following.

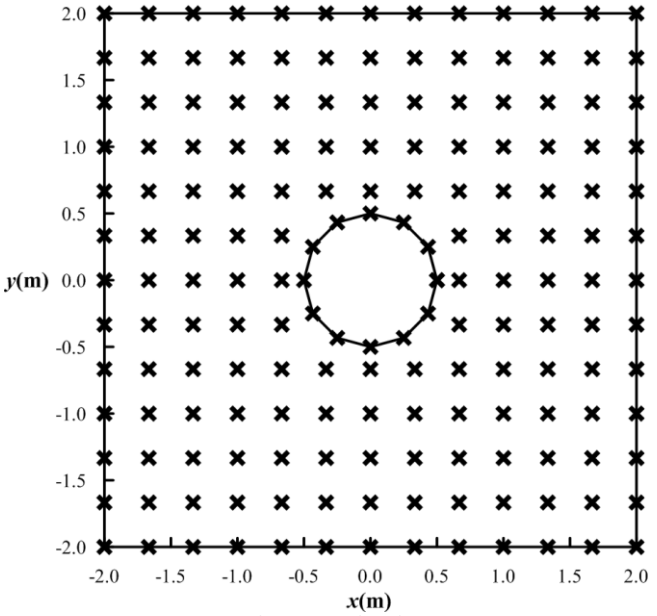

Fig. 1. Schematic configuration of uniformly distributed nodes.

To construct a linear equation for every node $\mathbf{y}_1$ and $\mathcal{L}^{\phi}$, we should approximate $\phi(\mathbf{x})$ around $\mathbf{y}_1$ by RBFs show in Fig. 2 as

$$\phi(\mathbf{x}) \approx \sum_{j=1}^{K} \alpha_j \chi(r_j), \tag{19}$$

where $r_j = \|\mathbf{x}-\mathbf{y}_j\|$ is the Euclidean distance from $\mathbf{x}$ to $\mathbf{y}_j$ and α_j is the corresponding undetermined coefficient. Here, $\mathbf{y}_j$'s are the positions of the K nearest neighbor nodes around the prescribed center $\mathbf{y}_i$. In this study, an algorithm based on kd-tree is employed to find the K nearest neighbor nodes efficiently (Bentley, 1975). Furthermore, the multiquadric RBF is written as

$$\chi(r_j) = \sqrt{r_j^2 + c^2}, \tag{20}$$

where c is the shape parameter (Hardy, 1971).

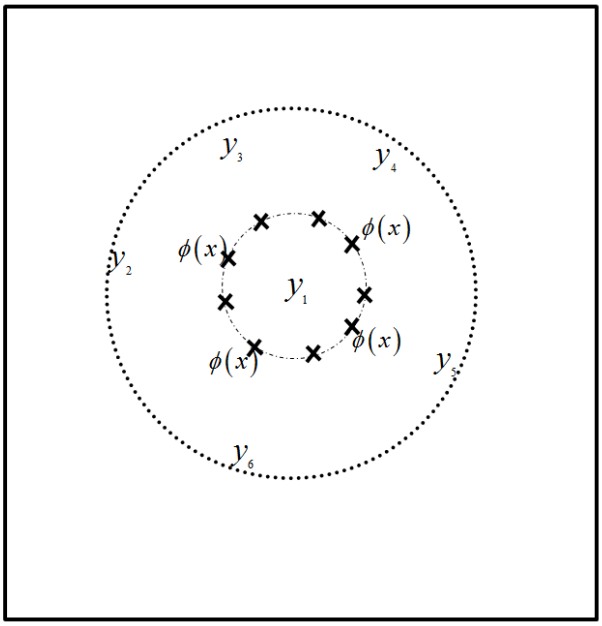

Fig. 2. Schematic configuration of approximate $\phi(\mathbf{x})$ around $\mathbf{y}_1$.

In order to circumvent the ill-conditioning problem for large K, a localization procedure proposed by the researchers (Liu et al., 2005a; Šarler and Vertnik, 2006; Lee et al., 2003) is introduced in the following. First, (19) is collocated on the K nearest neighbor nodes, then we have

$$\phi(\mathbf{y}_i) = \sum_{j=1}^{K} \alpha_j \chi\left(\|\mathbf{y}_i - \mathbf{y}_j\|\right) \text{ for } i = 1,...,K \tag{21}$$

which is in matrix-vector form as

$$\left[\phi\right]_{K\times 1} = \left[\chi\right]_{K\times K}\left[\alpha\right]_{K\times 1}, \tag{22}$$

where $\left[\phi\right]_{K\times 1}$ is defined in (18),

$$\left[\chi\right]_{K\times K} = \begin{bmatrix} \chi(\|\mathbf{y}_1-\mathbf{y}_1\|) & \chi(\|\mathbf{y}_1-\mathbf{y}_2\|) & \cdots & \chi(\|\mathbf{y}_1-\mathbf{y}_K\|) \\ \chi(\|\mathbf{y}_2-\mathbf{y}_1\|) & \chi(\|\mathbf{y}_2-\mathbf{y}_2\|) & \cdots & \chi(\|\mathbf{y}_2-\mathbf{y}_K\|) \\ \vdots & \vdots & \ddots & \vdots \\ \chi(\|\mathbf{y}_K-\mathbf{y}_1\|) & \chi(\|\mathbf{y}_K-\mathbf{y}_2\|) & \cdots & \chi(\|\mathbf{y}_K-\mathbf{y}_K\|) \end{bmatrix}, \tag{23}$$

and

$$\left[\alpha\right]_{K\times 1} = \begin{bmatrix} \alpha_1 \\ \alpha_2 \\ \vdots \\ \alpha_K \end{bmatrix}. \tag{24}$$

(22) can be inverted to have the resultant matrix form

$$\left[\alpha\right]_{K\times 1} = \left[\chi\right]^{-1}_{K\times K}\left[\phi\right]_{K\times 1}, \tag{25}$$

where $[\alpha]_{K\times 1}$ is the coefficient matrix.

Now, we consider $\mathcal{L}^{\phi}\phi(\mathbf{y}_i)$ for ϕ defined in (19). Here, $\mathcal{L}^{\phi}$ can be found in (13)~(16). Now, collocation of $\mathcal{L}^{\phi}\phi(\mathbf{x})$ on $\mathbf{y}_1$ gives

$$\mathcal{L}^{\phi}\phi(\mathbf{y}_1)=\sum_{j=1}^{K}\alpha_j\,\mathcal{L}^{\phi}\chi\left(\|\mathbf{x}-\mathbf{y}_i\|\right)\Big|_{\mathbf{x}=\mathbf{y}_1}, \tag{26}$$

or in matrix-vector form as

$$\mathcal{L}^{\phi}\phi(\mathbf{y}_1)=\left[\mathcal{L}^{\phi}\chi\right]_{1\times K}[\alpha]_{K\times 1}. \tag{27}$$

In (27), $\mathcal{L}^{\phi}\chi(r_j)$ is defined by

$$\left[\mathcal{L}^{\phi}\chi\right]_{1\times K} =\left[\mathcal{L}^{\phi}\chi\left(\|\mathbf{x}-\mathbf{y}_1\|\right)\Big|_{\mathbf{x}=\mathbf{y}_1}\quad\ldots\quad\mathcal{L}^{\phi}\chi\left(\|\mathbf{x}-\mathbf{y}_K\|\right)\Big|_{\mathbf{x}=\mathbf{y}_1}\right]. \tag{28}$$

Then, we combine (25) and (27) to have

$$\mathcal{L}^{\phi}\phi(\mathbf{x})\Big|_{\mathbf{x}=\mathbf{y}_i}=\left[\mathcal{L}^{\phi}\right]_{1\times K}[\phi]_{K\times 1}, \tag{29}$$

with

$$\left[\mathcal{L}^{\phi}\right]_{1\times K}=\left[\mathcal{L}^{\phi}\chi\right]_{1\times K}[\chi]^{-1}_{K\times K}. \tag{30}$$

In (29) and (30), it is clear that the row vector $\left[\mathcal{L}^{\phi}\right]_{1\times K}$ can be obtained if all of the $\mathcal{L}^{\phi}$, χ, and $\mathbf{y}_j$'s are known. This finish the local RBF approximation.

A. Operators on RBF

For completing the local RBF collocation method, we still need to explain the meaning of $\mathcal{L}^{\phi}$ for the operators given by $\nabla\cdot\mathbf{u}$, $\nabla(\nabla\cdot\mathbf{u})$, $\nabla\eta$, and $\mathbf{u}\cdot\nabla\mathbf{u}$. Without loss of generality, it is plausible to assume $\mathbf{y}_j=(0,0)$ and $r_j=r=\|\mathbf{y}\|$. Also, we need to define the following differential operator

$$\frac{D}{Dr}=\frac{d}{rdr}. \tag{31}$$

Then, we have

$$\frac{D\chi}{Dr}(r)=\frac{1}{\left(r^2+c^2\right)^{1/2}}, \tag{32}$$

$$\frac{D^2\chi}{Dr^2}(r)=\frac{-1}{\left(r^2+c^2\right)^{3/2}}. \tag{33}$$

Now, according to (13)~(16), we can summarize the five operators into the following two operators,

$$\frac{\partial\chi}{\partial x_i}=x_i\frac{D\chi}{Dr}=x_i\frac{1}{\sqrt{r^2+c^2}}, \tag{34}$$

and

$$\begin{aligned}\frac{\partial^2\chi}{\partial x_i\partial x_j}&=\left(\frac{\partial}{\partial x_i\partial x_j}\right)\chi\\&=\left(\left(\frac{D^2}{Dr^2}\right)x_ix_j+\delta_{ij}\frac{D}{Dr}\right)\chi\\&=x_ix_j\frac{1}{\sqrt{r^2+c^2}^{\,3}}+\delta_{ij}\frac{1}{\sqrt{r^2+c^2}}.\end{aligned} \tag{35}$$

Where χ, $\frac{D\chi}{Dr}$, $\frac{D^2\chi}{Dr^2}$ are given from (20), (32) and (33).

B. Time integration Scheme by Adams Predictor-corrector method

According to Wei and Kirby (1995), the Adams-Bashforth-Moulton predictor-corrector scheme issued to solve governing equations (1) and (2). This method includes predictor step and corrector step.

The predictor step is the third-order explicit Adams-Bashforth scheme given by

$$\{\eta\}^{n+1,0}=\{\eta\}^{n}+\frac{\Delta t}{12}\left(23\{E\}^{n}-16\{E\}^{n-1}+5\{E\}^{n-2}\right), \tag{36}$$

$$\{\mathbf{u}\}^{n+1,0}=\{\mathbf{u}\}^{n}+\frac{\Delta t}{12}\left(23\{\mathbf{F}\}^{n}-16\{\mathbf{F}\}^{n-1}+5\{\mathbf{F}\}^{n-2}\right)+2\{\mathbf{F}_1\}^{n}-3\{\mathbf{F}_1\}^{n-1}+\{\mathbf{F}_1\}^{n-2}, \tag{37}$$

where E, $\mathbf{F}$ and $\mathbf{F}_1$ are functions of η, u and v. All information on the right is known from previous calculations.

After the predicted values are evaluated, we obtain the corresponding spatial derivative $\{\eta\}^{n+1,0}$ and $\mathbf{U}^{n+1,0}$.

The corrector scheme is the fourth-order Adams-Moulton method, given by

$$\{\eta\}^{n+1,s+1}=\{\eta\}^{n}+\frac{\Delta t}{24}\left(9\{E\}^{n+1,s}+19\{E\}^{n}-5\{E\}^{n-1}+\{E\}^{n-2}\right), \tag{38}$$

$$\{\mathbf{u}\}^{n+1,s+1}=\{\mathbf{u}\}^{n}+\frac{\Delta t}{24}\left(9\{\mathbf{F}\}^{n+1,s}+19\{\mathbf{F}\}^{n}-5\{\mathbf{F}\}^{n-1}+\{\mathbf{F}\}^{n-2}\right)+\{\mathbf{F}_1\}^{n+1,s}-\{\mathbf{F}_1\}^{n}. \tag{39}$$

The corrector step is iterated until the error between two successive results reaches a required limit. The error is computed for each of the three dependent variables η, u and v are defined as

$$\frac{\sum_i\left|f_i^{n+1,s+1}-f_i^{(n+1),s}\right|}{\sum_i f_i^{n+1,s+1}}<0.001, \tag{40}$$

where $f_i=\eta_i$ or $\mathbf{u}_i$ stand for any of the variables and

$(\ )^*$ express the previous estimate. When the equation reaches convergence (40) as

$$f_i^{n+1} = f_i^{n+1,s+1}, \tag{41}$$

f_i is the variable value at i-th discretized spatial point x_i

C. Boundary conditions

In numerical models, suitable boundary conditions are needed. Three types of boundary conditions in this study.

These are (1) Reflective boundaries. (2) Internal generation of waves. (3) Absorbing boundary condition.

1) Reflective boundaries

The kinematic boundary condition at an impermeable wall are given as

$$\mathbf{u}\cdot\mathbf{n} = 0 \qquad \mathbf{x}\in\partial\Omega, \tag{42}$$

$$\frac{\partial\eta}{\partial n} = 0 \qquad \mathbf{x}\in\partial\Omega, \tag{43}$$

where $\mathbf{n}$ is an outward normal vector, Ω is the fluid domain; $\partial\Omega$ is the boundary; $\mathbf{x}$ is a position in the boundary.

The velocity component $u\cdot T$ notation tangent to the boundary, we require

$$\frac{\partial(u\cdot T)}{\partial n} = 0 \qquad \mathbf{x}\in\partial\Omega. \tag{44}$$

This last condition essentially imposes a no-shear condition for the flow along the bounding wall, which is not inconsistent with the inviscid flow being considered.

2) Internal generation of waves

Wei et al. (1990) proposed to generate the internal wave on a constant water depth need that adding a source term $f(x,y,t)$ in the continuity equation.

The source function $f(x,y,t)$ can be written as follows:

$$f(x,y,t) = \frac{2a_0\cos(\theta)\left(\omega^2-\xi_1 gk^4h^3\right)}{\omega k I\left[1-\xi(kh)^2\right]}\sin(k_y y-\omega t)\times\exp[-\beta_0(x-x_c)^2], \tag{45}$$

where a_0 is the wave amplitude; ω is the wave frequency; k is wave number; x_c is the central location of source in the x-direction; $k_y = k\sin(\theta)$ is the wave number in the y-direction; ξ and ξ_1 are coefficient and I given by

$$\xi = \frac{z_\alpha}{h}\left(\frac{1}{2}\frac{z_\alpha}{h}+1\right); \quad \xi_1 = \alpha+1/3, \tag{46}$$

$$I = \sqrt{\frac{\pi}{\beta_0}}\exp\left(-k_x^2/4\beta_0\right), \tag{47}$$

where $k_x = k\cos(\theta)$ is the wave number in the x-direction and source width parameter β_0 is given by

$$\beta_0 = \frac{80}{\delta^2 L^2}, \tag{48}$$

where the value of δ we use in the model is in the range of 0.3-0.5 and L is the wavelength.

3) Absorbing boundary condition

When the waves are transmitted to the open boundary, the absorbing boundary condition can effectively absorb the wave energy in order to avoid reflection waves occurred. The wave phase speed c and the propagation direction θ at the boundary are known, the radiation condition is

$$\eta_t + c\cos\theta\eta_x = 0. \tag{49}$$

For two-dimensional applications, the approximate radiation boundary condition can be written

$$\eta_{tt} + c\eta_{xt} - \frac{c^2}{2}\eta_{yy} = 0. \tag{50}$$

To reduce the reflection, a damping layer is applied to the computing domain. Damping terms are added to the momentum equations as

$$\mathbf{u}_t = \mathbf{F}(\eta,\mathbf{u}) + \left[\mathbf{F_1}(\mathbf{u})\right]_t - w_1(x)\mathbf{u} - w_2(x)\left(\mathbf{u}_{xx}+\mathbf{u}_{yy}\right), \tag{51}$$

where the damping terms are called "Newtonian cooling" of $\mathbf{u}$. The damping coefficients $w_1(x)$ and $w_2(x)$ are defined as

$$w_1(x) = \begin{cases} 0; & x < x_s \\ \alpha_1\omega f(x); & x > x_s \end{cases} \tag{52}$$

$$w_2(x) = \begin{cases} 0; & x < x_s \\ \alpha_2\nu f(x); & x > x_s \end{cases} \tag{53}$$

where α_1 and α_2 are free parameters to be determined in the numerical calculations, w is frequency of wave to be damped; x_s is starting coordinate of damping layer (the computing domain is from $x=0$ to $x=x_l$); ν is viscous coefficient; $f(x)$ is defined as

$$f(x) = \frac{\exp\left(\dfrac{x-x_s}{x_1-x_s}\right)^n - 1}{\exp(1)-1}, \tag{54}$$

where n is constant to be determined for the specific running. The damping layer width usually takes the wave length two time or three times. The numerical experiment indicated that, adding damping layer with radiation boundary condition, the effect is good than radiation conditions alone.

IV. NUMERICAL RESULTS AND DISSCUSSION

In this section, two cases of two-dimensional problems were verified. We use the LRBFCM discretization of the corresponding governing equations.

A. Regular wave propagation in a channel

In order to determine the feasibility of wave generation method in our model. We first use the wave generation to make the regular waves in a channel which is with a length of 20.0 m, width of 1.0 m and constant water depth h = 0.1 m. For instance, the expected generated wave height is 0.005 m and the period is 1.0 s. The grid size used in the model is $\Delta x = 0.04$ m and the time step is $\Delta t = 0.02$ s. The center of the source region is located at $x = 10$ m and the sponge layer at the two ends boundaries to absorb the waves effectively. Fig. 3 showing the surface elevation at different times.

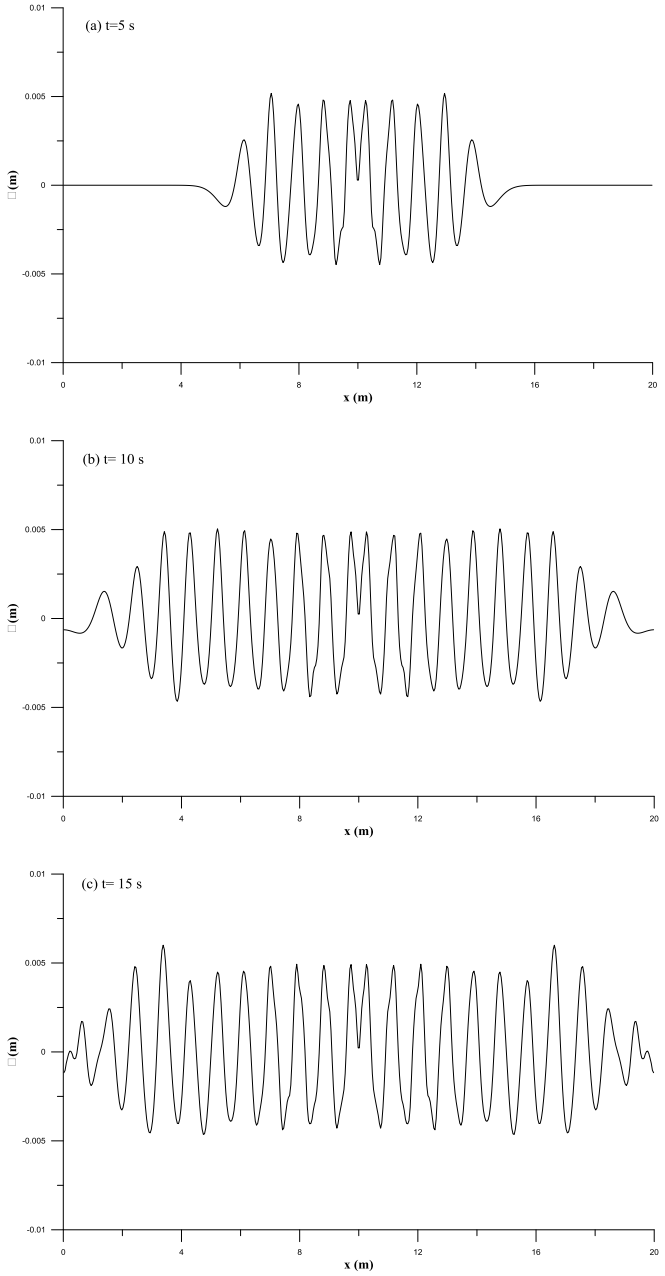

Fig. 3. The internally generated free-surface elevation of regular waves : (a) 5s; (b) 10s; (c) 15s.

B. Wave evolution in a rectangular basin

To substantiate the 2D numerical model in cases, we apply evolution in Closed Rectangular in a closed basin. The two-dimensional domain of the size $(L_x = 10) \times (L_y = 10)$ m. The boundary in around set the reflective vertical walls. In the center of the basin that the initial free surface displacement being Gaussian distribution:

$$\eta_0(x, y) = H_0 \exp\left\{-\gamma\left[\left(x - L_x/2\right)^2 + \left(y - L_y/2\right)^2\right]\right\}, \quad (55)$$

where H_0 is the initial height of the wave and γ is the crest increase element, the variation of free surface in the basin was provided the linear analytical solution by Wei and Kirby (1995).

$$\eta(x, y, t) = \sum_{n=0}^{\infty}\sum_{m=0}^{\infty} \bar{\eta}_{nm} e^{-i\omega_{nm}t} \cos(n\lambda x)\cos(m\lambda y), \quad (56)$$

in which

$$\bar{\eta}_{nm} = \frac{4}{(1+\delta_{n0})(1+\delta_{m0})L_x L_y}\int_0^{Lx}\int_0^{Ly} \eta_0(x, y)\cos(n\lambda x)\cos(m\lambda y)\,dxdy, \quad (57)$$

where δ_{nm} is the Kronecker delta function and

$$\lambda = \frac{\pi}{L_x} = \frac{\pi}{L_y}. \quad (58)$$

The (n, m) wave modes has the relevant natural frequency that is given by the linear dispersion equation,

$$\omega_{nm}^2 = g k_{nm} \tanh(k_{nm} h_0), \quad (59)$$

where h_0 is the constant water depth and

$$k_{nm}^2 = (n\lambda)^2 + (m\lambda)^2 = \left(\frac{\pi}{L_x}\right)^2 (n^2 + m^2). \quad (60)$$

In this example, the parameters are defined as $h_0 = 0.5$ m, $H = 0.1$, and $\gamma = 0.4$. The domain of this case, we use uniform grids with $\Delta x = \Delta y = 0.2$ and the time step of $\Delta t = 0.05$ was run for 50 s. In principle, we neglect the loss of energy. The results of the numerical simulation can be observed that symmetric waveforms are preserved in Fig. 4. Fig. 5 shown snapshots of the free surface evolution.

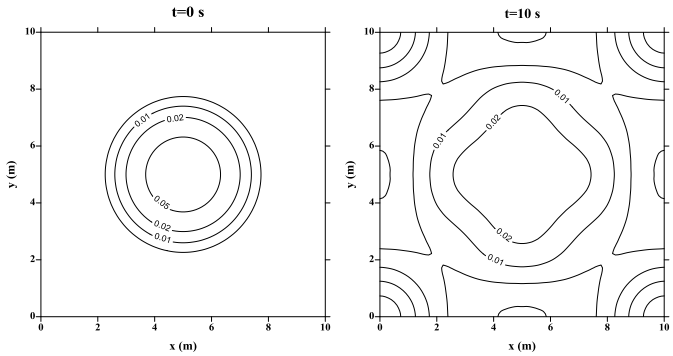

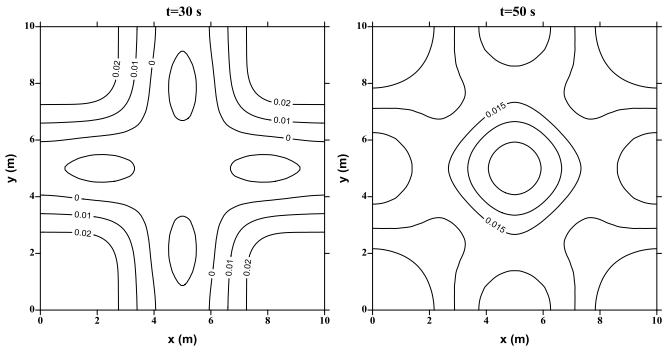

Fig. 4. Contour plots of η at $t = 0, 10, 30$ and 50 s in Closed Rectangular Basin for $H = 0.1$ m.

To further verify the applicability and validity of the present model that we compare a series of numerical analysis similar to the above problem with $H_0 = 0.005$, 0.05 and 0.2 m.

These three studies including linear, weakly nonlinear and strong nonlinear wave problems, respectively. The time series of free surface elevation at the wave basin is gained from the numerical models' results and compared to the linear theory (Wei and Kirby, 1995) at the $\eta = (1,1)$ m and at the center of the basin. Figs. 6, 7 and 8 show comparison of numerical results (dashed line) and linear analytical solution (solid line) for the 50 s after the release of the elevation.

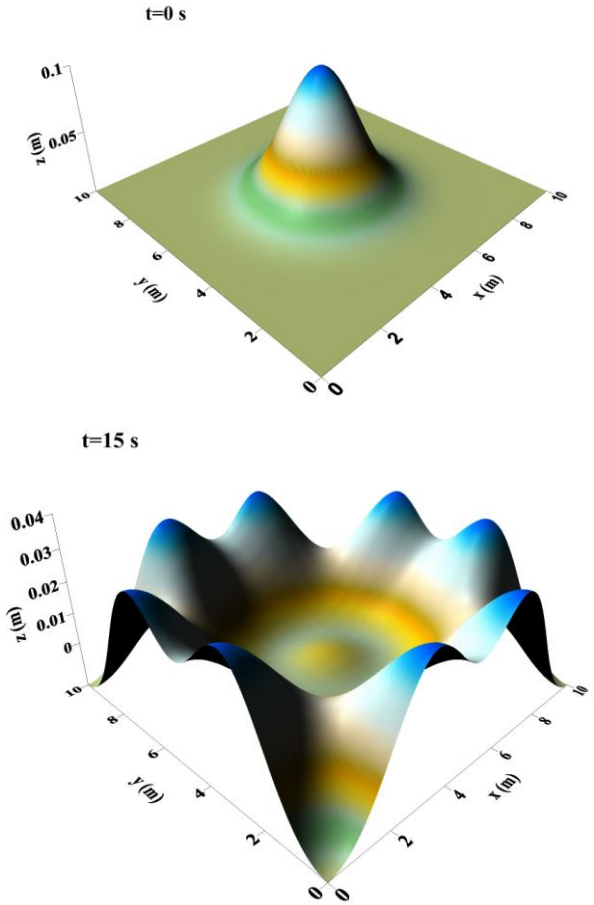

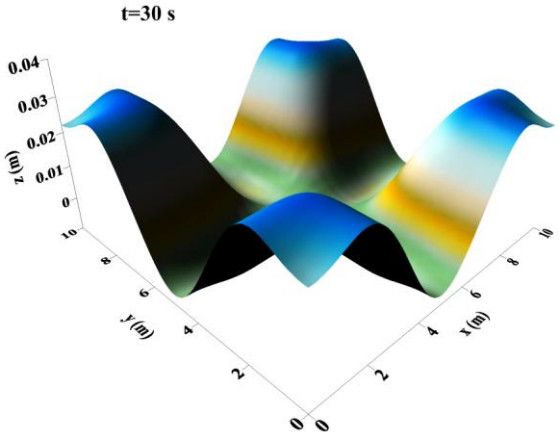

Fig. 5. Linear Gaussian-wave profiles at three different times.

It is obvious that the numerical results for the considered three cases are very close to each other. Fig. 6 shows such comparisons for $H_0 = 0.005$ m. It is seen that almost similar matches are obtained among the linear theory, especially in the first 20 seconds. With the increase of wave height, we can more easily notice that the effect of wave nonlinear. When $H_0 = 0.05$ m, Fig. 7 shows the weakly nonlinear consequence.

As for cases $H_0 = 0.2$ m, because the wave height is relatively large, the effect of wave nonlinearity is stronger. It is distinct deviate the linear wave theory after 10 seconds. The result of the comparison is shown in Fig. 8.

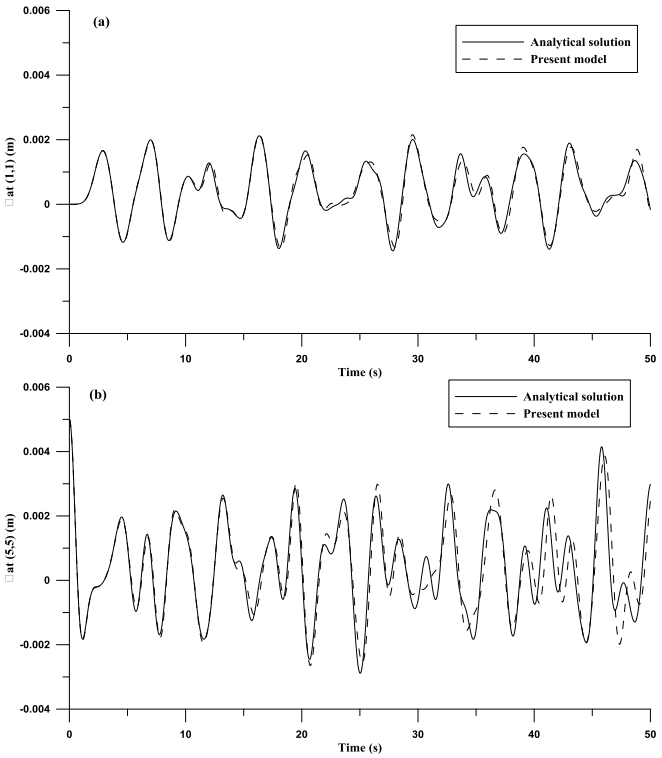

Fig. 6. Free surface time history at (a) $\eta = (1,1)$ m and (b) the center of the basin with the present numerical and linear analytical solution for $H_0/h_0 = 0.01$

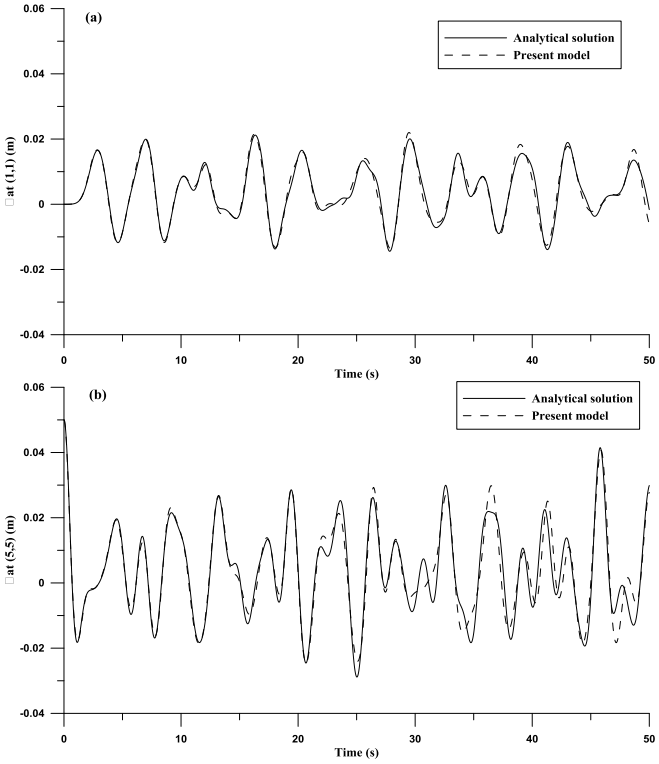

Fig. 7. Free surface time history at (a) $\eta = (1,1)$ m and (b) the center of the basin with the present numerical and linear analytical solution for $H_0/h_0 = 0.1$

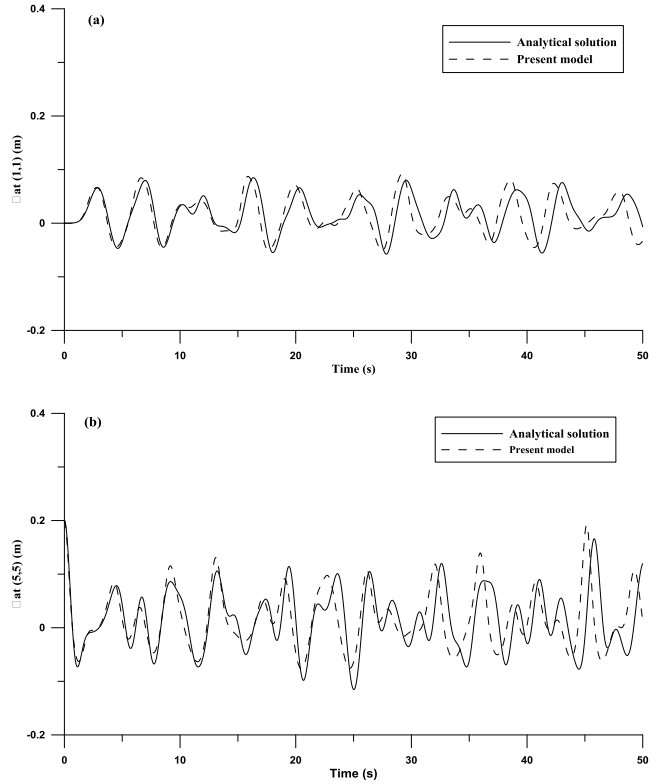

Fig. 8. Free surface time history at (a) $\eta = (1,1)$ m and (b) the center of the basin with the present numerical and linear analytical solution for analytical solution for $H_0/h_0 = 0.4$

V. CONCLUSION

The Boussinesq equations are able to describe the propagation of the wave in the nearshore. The theory of Boussinesq equations has the different types, which are relevant to different horizontal velocities and higher-order terms. In this paper, an approximation method of LRBFCM on the extended Boussinesq equations derived by Nwogu (1993) is developed. It is a brand-new combination of wave transmission. The time marching is performed using the fourth-order Adams–Bashforth–Moulton predictor and corrector scheme. The local radial-basis-function collocation method presents a useful alternative to solve the problems in engineering. The main concept of LRBFCM is the interpolation function values only associated with the neighboring nodes in the entire domain. In contrast to the fully dense matrices with the global methods, the localized approach leads to sparse matrices which could increase the computation efficiency. We used the multiquadric radial basis function in this study. Therefore, we have a preliminary verification of our model. Two 2D cases in this paper include regular wave propagation in a channel and regular wave evolution in a rectangular basin. The numerical results are quite similar compared with analytical theory. Even though the error of strong nonlinear effect is visible, the model is feasibility in the performance of other results.

We are currently comparing different 2D cases and trying to add fully non-linear terms (Wei et al., 1995) in our model. We will be proposed elsewhere.

ACKNOWLEDGMENT

The Ministry of Science and Technology of Taiwan is gratefully acknowledged for providing financial support to carry out the present work under the Grant No. MOST 105-2221-E-022-019-039-MY3.

REFERENCES

[1] Abbott, M., H. Petersen, and O. Skovgaard, On the numerical modelling of short waves in shallow water. Journal of Hydraulic Research, 1978. 16(3): p. 173-204.

[2] Bentley, J.L., Multidimensional binary search trees used for associative searching. Communications of the ACM, 1975. 18(9): p. 509-517.

[3] Boussinesq, J., Theorie des ondes et des remous qui se propagent le long d'un canal rectangulaire horizontal, en communiquant an liquide contenu dans ce canal de vitesses sensiblement pareilles de la surface anfond, Liouvilles. J. Math., 1872. 17: p. 55-108.

[4] Cienfuegos, R., E. Barthélemy, and P. Bonneton, A fourth-order compact finite volume scheme for fully nonlinear and weakly dispersive Boussinesq-type equations. Part I: model development and analysis. International Journal for Numerical Methods in Fluids, 2006. 51(11): p. 1217-1253.

[5] Erduran, K., S. Ilic, and V. Kutija, Hybrid finite-volume finite-difference scheme for the solution of Boussinesq equations. International Journal for Numerical Methods in Fluids, 2005. 49(11): p. 1213-1232.

[6] Hardy, R.L., Multiquadric equations of topography and other irregular surfaces. Journal of Geophysical Research, 1971. 76(8): p. 1905-1915.

[7] Kansa, E.J., Multiquadrics—A scattered data approximation scheme with applications to computational fluid-dynamics—I surface approximations and partial derivative estimates. Computers & Mathematics with Applications, 1990. 19(8-9): p. 127-145.

[8] Kansa, E.J., Multiquadrics—A scattered data approximation scheme with applications to computational fluid-dynamics—II solutions to parabolic, hyperbolic and elliptic partial differential equations. Computers & Mathematics with Applications, 1990. 19(8-9): p. 147-161.
[9] Katopodes, N.D. and C.-T. Wu, Computation of finite-amplitude dispersive waves. Journal of Waterway, Port, Coastal, and Ocean Engineering, 1987. 113(4): p. 327-346.
[10] Kosec, G. and B. Sarler, Local RBF collocation method for Darcy flow. Computer Modeling in Engineering and Sciences, 2008. 25(3): p. 197.
[11] Kosec, G., et al., A meshless approach towards solution of macrosegregation phenomena. Computers, Materials, & Continua, 2011. 22(2): p. 169-195.
[12] Lee, C.K., X. Liu, and S.C. Fan, Local multiquadric approximation for solving boundary value problems. Computational Mechanics, 2003. 30(5-6): p. 396-409.
[13] Li, Y., et al., Numerical modeling of Boussinesq equations by finite element method. Coastal Engineering, 1999. 37(2): p. 97-122.
[14] Liu, X., et al., Radial point interpolation collocation method (RPICM) for partial differential equations. Computers & Mathematics with Applications, 2005. 50(8-9): p. 1425-1442.
[15] Liu, X., et al., Radial point interpolation collocation method (RPICM) for the solution of nonlinear Poisson problems. Computational Mechanics, 2005. 36(4): p. 298-306.
[16] Madsen, P.A. and O.R. Sørensen, A new form of the Boussinesq equations with improved linear dispersion characteristics. Part 2. A slowly-varying bathymetry. Coastal Engineering, 1992. 18(3-4): p. 183-204.
[17] Nwogu, O., Alternative form of Boussinesq equations for nearshore wave propagation. Journal of Waterway, Port, Coastal, and Ocean Engineering, 1993. 119(6): p. 618-638.
[18] Peregrine, D.H., Long waves on a beach. Journal of Fluid Mechanics, 1967. 27(4): p. 815-827.
[19] Šarler, B. and R. Vertnik, Meshfree explicit local radial basis function collocation method for diffusion problems. Computers & Mathematics with Applications, 2006. 51(8): p. 1269-1282.
[20] Tonelli, M. and M. Petti, Hybrid finite volume–finite difference scheme for 2DH improved Boussinesq equations. Coastal Engineering, 2009. 56(5-6): p. 609-620.
[21] Tsai, C.C., Lin Z.H,. Hsu T.W. Using a local radial basis function collocation method to approximate radiation boundary conditions. Ocean Engineering, 2015, 105, 231-241.
[22] Wei, G. and J.T. Kirby, Time-dependent numerical code for extended Boussinesq equations. Journal of Waterway, Port, Coastal, and Ocean Engineering, 1995. 121(5): p. 251-261.
[23] Wei, G., et al., A fully nonlinear Boussinesq model for surface waves. Part 1. Highly nonlinear unsteady waves. Journal of Fluid Mechanics, 1995. 294: p. 71-92.
[24] Wei, G., J.T. Kirby, and A. Sinha, Generation of waves in Boussinesq models using a source function method. Coastal Engineering, 1999. 36(4): p. 271-299.
[25] Zelt, J. and F. Raichlen, A Lagrangian model for wave-induced harbour oscillations. Journal of Fluid Mechanics, 1990. 213: p. 203-225.